Time-frequency microstructure of event-related EEG desynchronization and synchronization.

Piotr J. Durka*, Dobiesław Ircha*, Christa Neuper§ Gert Pfurtscheller¶

Medical & Biological Engineering & Computing, Vol. 39, No. 3, May 2001, © IEE

Abstract

We present a new method for analysis of event-related EEG phenomena, in particular ERD/ERS related to a voluntary movement, which offers:

- high time-frequency resolution, and hence also increased ERD/ERS sensitivity (especially in the gamma band, where improvement may exceed order of magnitude),
- possibility to analyze the whole picture of energy changes at once, without setting *a priori* the analyzed frequency bands,
- parametric description of signal's structures.

The main idea is based upon averaging energy distributions of single EEG trials in the time-frequency plane. As the estimator for signal's energy density we choose matching pursuit with stochastic Gabor dictionaries. Other possible estimates are presented on simulated signal and discussed briefly. Consistence of results with previous findings is evaluated on the data from a classical voluntary finger movement experiment.
Keywords: ERD, ERS, ERP, gamma activity, time-frequency, matching pursuit.

*Laboratory of Medical Physics, Warsaw University, ul. Hoża 69, 00-681 Warszawa, Poland. This work was supported by Polish State Committee for Scientific Research grant 8T11E014016.

§Ludwig Boltzmann Institute of Medical Informatics and Neuroinformatics, Graz University of Technology

¶Department of Medical Informatics, Institute for Biomedical Engineering, Graz University of Technology, Inffeldgasse 16a, A-8010 Graz, Austria. This work was supported by the "Austrian Fonds zur Förderung der wissenschaftlichen Forschung" (Project 12407)

1 Introduction

Populations of neurons can form complex neuronal networks whereby feedback loops are responsible for the generation of oscillatory activity and determine its resonance frequency. In general, the frequency becomes slower and the amplitude larger with increasing extent of synchronized neuronal assemblies [12]. Even if only a small fraction of the total population of neurons is synchronized, the resulting oscillations may well overweight the rest of not-synchronized neurons [4].

Because of the great complexity, reciprocal interactions between excitatory and inhibitory mechanisms and dynamics of neural networks in sensorimotor areas, not only one but a great variety of oscillations in a broad frequency range exists. These networks can be in different states depending on the level of sensorimotor information processing. So for example during immobility or rest, a 10-Hz Rolandic rhythm (mu rhythm) dominates in most cases [5]. In the phase of planning e.g. a voluntary finger movement, the mu rhythm desynchronizes [9]. This means that more and more patches of neurons start to work independently and the number of coherently activated neurons as well as the amplitudes of the oscillations decrease. Shortly before the actual movement begins, small groups of neurons, becoming synchronously activated, may result in oscillations around 40 Hz (gamma activity). After termination of movement, oscillations around 20 Hz are found. Both the oscillations in beta and gamma bands are embedded in the desynchronized 10-Hz [8, 9].

For a better understanding of cortical functioning and the significance of oscillations with distinct frequencies, it is important to investigate frequency, latency and duration of oscillatory bursts as accurately as possible. The gamma oscillations are of special importance because they may serve as cortical information carrier and are essential for establishing of rapid coupling between spatially separated cell assemblies [12].

Traditionally, the time course of frequency-specific changes of energy was quantified by band-pass filtering of signals in a chosen frequency band. Drawbacks of this approach include *a priori* choice of the frequency bands (usually by certain trial-and-error procedure), low resolution, and low selectivity to phenomena originating in given frequency band. This paper introduces a complete methodology for a high-resolution presentation and parametrization of event-related EEG in the time-frequency plane. Estimates of energy density are based upon the matching pursuit algorithm [6] with recently introduced stochastic dictionaries [3] (a brief comparison with some other time-frequency distributions is presented on a simulated signal). Owing to the direct parametrization of signal's structures, this approach allows also for construction of selective estimators of energy carried by structures originating in a given frequency band.

2 Experimental data

Human subjects displaying, beside mu and beta rhythms, clear movement-related gamma oscillations in the EEG are rare. In the last years we had only 3 subjects displaying significant enhancement of gamma oscillations in a self-paced movement task. Especially one of them showed unusually prominent 40-Hz EEG activity during movements, and therefore he participated in a series of EEG studies performed to investigate this 40-Hz activity in more detail [8, 9, 10]. Results of MEG measurements for the same subject were reported in [11]. EEG data of this subject was chosen to study the performance of the proposed method.

2.1 Procedure

The data of one subject (male, right-handed, 29 years old) who reliably has displayed 40-Hz oscillations prior to movement (previously reported in [9]) was used for the present EEG data analyses. During the voluntary movement experiment the subject performed about 100 brisk extension and flexion movements of the right index finger in intervals not shorter than 12 s.

2.2 EEG recording

EEG was recorded from 56 Ag/AgCl electrodes placed 2.5 cm apart in a grid overlying central and related regions (see insert in Fig. 3). The amplifier upper frequency limit was 50 Hz, the time constant 1 s, and the sampling frequency 128 Hz. The reference electrode was mounted on the right ear and the grounding electrode on the forehead. EOG was recorded from the lateral corners of both eyes. Surface EMG was recorded from the right forearm (m. extensor digitorum communis) with 1 kHz upper frequency limit and 0.1 s time constant. EMG was rectified and full-wave integrated by a contour follower time constant of 0.04 s (see [9]). A photo-electric sensor was placed on the tip of the index finger to indicate onset and offset of movements.

2.3 EEG preprocessing

All EEG data were visually controlled for EOG and EMG artifacts and affected epochs were excluded. For each movement, a 10 s-epoch (5 s before, 5 s after movement-onset) was analyzed. Reference-free EEG data were obtained by computing the local average reference [13]. For analysis reported in this paper only data (referential and local average) of one electrode position over the left sensorimotor region (located 2.5 cm posterior and 2.5 cm medial to C3, see Fig. 3) was selected, since it revealed maximal reactivity in the frequency range around 40 Hz.

3 Methods

3.1 Conventional ERD/ERS quantification

Event-related desynchronization (ERD) and event-related synchronization (ERS) is the change of signal's power occuring in a given band, relative to a reference interval, in this experiment chosen between 4.5 and 3.5 seconds before the movement onset. Movement-reactive frequency components were detected by comparing power spectral densities in the reference interval (-4.5 s to -3.5 s) and in a 1 s-period around the movement (-0.5 to +0.5

s). Frequency bands, showing significant differences between the reference interval and the activity interval, were chosen for ERD/ERS computations. The EEG was digitally band pass filtered in the selected bands (alpha band 10-12 Hz; beta band 14-18 Hz; gamma band 36-40 Hz) and power values were computed by squaring the samples and averaging these power samples across trials. To reduce the number of power values (original signal was sampled 128Hz), 16 consecutive samples were averaged producing an 8 Hz sampling rate in the resulting power time series. Absolute band power was converted to percentage power using the reference interval as 100%. By convention, an ERD corresponds to power decrease and an ERS to a power increase [7]. Results are presented in Figure 3.

3.2 Matching pursuit

Matching Pursuit (MP) is an iterative procedure, proposed by Mallat and Zhang [6] in 1993. In the first step of MP, the waveform g_{γ_0} which best matches the signal $f(t)$ is chosen from a large and redundant set (a dictionary). In each of the consecutive steps, waveform g_{γ_n} is matched to the signal $R^n f$, which is the residual left after subtracting results of previous iterations:

$$\begin{cases} R^0 f = f \\ R^n f = < R^n f, g_{\gamma_n} > g_{\gamma_n} + R^{n+1} f \\ g_{\gamma_n} = \arg\max_{g_{\gamma_i} \in D} | < R^n f, g_{\gamma_i} > | \end{cases} \quad (1)$$

Orthogonality of $R^{n+1} f$ and g_{γ_n} in each step implies energy conservation:

$$||f||^2 = \sum_{n=0}^{m-1} | < R^n f,\ g_{\gamma_n} > |^2 + ||R^m f||^2 \quad (2)$$

For a complete dictionary the procedure converges to f:

$$f = \sum_{n=0}^{\infty} < R^n f,\ g_{\gamma_n} > g_{\gamma_n} \quad (3)$$

Results of the above procedure depend on the set of functions available for the decomposition, i.e. the dictionary. We use Gabor functions (sine-modulated Gaussian), which provide optimal joint time-frequency localization. A real Gabor function can be expressed as:

$$g_\gamma(t) = K(\gamma) e^{-\pi \left(\frac{t-u}{s}\right)^2} \sin\left(\omega(t-u) + \phi\right) \quad (4)$$

$K(\gamma)$ is such that $||g_\gamma|| = 1$. $\gamma = \{u, \omega, s, \phi\}$ denotes parameters of possible dictionary's functions (time-frequency atoms).

However, within ranges of these continuous parameters no particular sampling is *a priori* defined, so we are confronted with a potentially infinite dictionary size. Therefore, in practical implementations, we use subsets of the possible dictionary functions. In choosing such subset, any fixed subsampling of the parameter space introduces a statistical bias in the resulting parametrization. Free of bias parametrization is possible with stochastic dictionaries, where the parameters of a dictionary's atoms are randomized before each decomposition. Further details can be found in [3].

In general, mathematics related to the non-linear MP algorithm can be quite complicated. Nevertheless, for a reasonable application if its results, it is basically enough to understand that structures present in the signal are explained in terms of functions g_{γ_i} (equation (3)), chosen for its representation from the dictionary. In case of the Gabor dictionary, each of these structures will be described by it's time and frequency positions, time spread, amplitude and phase.

3.3 Time-frequency distribution of signal's energy

Expansion (3) can be used to construct a time-frequency map of signal's energy, which is a priori free of cross terms.

Energy is a quadratic function of the signal. If we have signal composed of structures a and b, then its square gives $(a+b)^2 = a^2 + b^2 + 2ab$. In most of the time-frequency distributions, cross-terms ($2ab$) may have up to twice the energy of terms directly related to signal's structures, but appear at time and frequency positions where no activity occurs in the signal. Sophisticated mathematics is being applied to reduce the cross-terms, resulting in a multitude of distributions: each of them may produce a better picture for certain signal. Their variety, combined with the complex multi-component character of EEG, requires a careful choice of a proper analysis method and its parameters for each experimental setup.

But once we managed to decompose the signal into linear expansion (3), total elimination of cross-terms is trivial. We simply omit all the mixed elements appearing in the square of the right side, leaving sum of Wigner distributions of M auto-terms g_{γ_n} [6]:

$$Ef(t,\omega) = \sum_{n=0}^{M} | < R^n f,\ g_{\gamma_n} > |^2 \ W g_{\gamma_n}(t,\omega) \quad (5)$$

This estimate is derived from a general procedure, which does not require a signal-dependent tuning, and conserves high resolution of the underlying parametrization (eq. 3). Figure 1 (f) presents this magnitude calculated for a simple signal simulated as a sum of typical components.

Figure 2 presents time-frequency distributions of energy of a simulated signal from Figure 1, obtained by means of several different methods. Spectrograms (short-time Fourier transform) from plots (b) and (c) indicate the tradeoff between time and frequency resolutions, inherent to this distribution. It is regulated by the length of the time window—its average setting gives usually rather low overall resolution, with minimized cross-terms. Plot (d) represents the continuous wavelet transform, indicating its most typical property: time resolution changing proportionally with the frequency, e.g. good time and bad frequency resolutions in the high frequency region. Finally, plot (e) and its 3-dimensional representation in (f) are obtained from a pseudo smoothed Wigner-Ville distribution, with separable parameters governing time and frequency resolutions. These parameters were chosen to optimize the representation of all the structures present in this signal, at a cost of incorporating relatively low-energy interferences (cross-terms).

Neither this figure alone, nor its comparison with Figure 1, is intended as a proof of a total superiority of one method. For each type or even instance of a signal, different distributions may exhibit specific advantages. The conclusion, important in the context of this paper, is that results provided by time-frequency distributions heavily depend on the particular choice of the method and its parameters. On the contrary, MP decomposition offers one of the highest possible resolutions in most of the cases—provided that Gabor functions describe well the analyzed signal, assumption which usually holds for EEG. Performance of the procedure can be significantly distorted only if we apply an unproportionally small dictionary. Although there is still no golden rule for a proper choice of "large enough" dictionary's size[1], practical experience in this respect is rapidly gained and applicable to a wide classes of signals. Another free parameter in the MP decomposition is the number of iterations (i.e. waveforms in expansion (3)), but this can be regulated by a requirement of explaining a given percentage of signal's energy.

Averaging signal's energy density in the time-frequency plane

Time-frequency distribution (map) of signal's energy density contains no information about the phase of signal's structures. We estimate this magnitude—by means of the the MP procedure described in the previous sections—separately for all the single trials, and then average resulting maps. Such an average (Figures 4–6) enhances structures bearing similar time-frequency signatures—i.e. occurring in the same time-frequency region, as related to the trigger—irrelevant of their phase relations. Contrary to the averaging in the time domain, it allows to pick from noise also those phenomena, where phase synchronization does not occur, or, as in high frequencies, can be distorted by limited accuracy of the trigger's time localization. This approach was briefly presented at a conference [2].

4 Results

4.1 Classical results

Fig. 3 depicts the ERD/ERS time courses for the 10-12, 14-18 and 36-40 Hz bands. The alpha band (mu) desynchronization (10-12 Hz) starts 2.5 s before movement-onset, reaches maximal desynchronization shortly after movement-onset and recovers to baseline level within a few seconds. The central beta activity (14-18 Hz), in contrast, displays a short-lasting ERD during initiation of movement followed by a synchronization (ERS) with a maximum after the movement execution. It is of interest

[1]Further increasing the size of a dictionary used for MP decomposition does not deterior the quality of decomposition—on the contrary, in theory the resolution grows with its size, but starting from certain values this effect is hard to notice. The problem is that the algorithm requires large computational resources—time and memory—proportional to the size of applied dictionary.

that the beta ERS occurs while the mu rhythm still shows a desynchronization. The 40-Hz oscillations (36-40 Hz) reveal a sharp power increase shortly before movement-onset.

4.2 New results

Average time-frequency maps of energy density of EEG responses (Figures 5, 6) were obtained as follows:

1. Single trials from the data described in chapter 2 were subjected to MP decomposition in stochastic Gabor dictionaries.

2. For each trial, a time-frequency map of signal's energy density was constructed. Time-frequency structures of duration below 0.125 sec. were excluded from the maps—this can be understood as a kind of non-linear denoising, and corresponds to smoothing in time curves from Figure 3 by 16-points window. Parallel procedure (exclusion of structures longer than 4 sec.) was used to remove sharp frequency artifacts.

3. Finally, all the time-frequency maps constructed for single trials were added, to produce an average (across trials) distribution of signal's energy in the time-frequency plane (Figures 5 and 6).

Slices corresponding to the frequency bands used in classical ERD/ERS quantification (section 3.1) were cut from this distribution in Figure 4. Curves presented above those slices are corresponding frequency integrals. Value at each point of a curve is a sum of energies at this time point for all the frequencies in given band, i.e. from the the map below.

Parametric description of signal structures opens also amazing possibilities of signal analysis in the space of parameters of functions from the signal's expansion (3). As an example, Figure 7 presents estimation of the energy carried by structures with frequency centers lying within certain interval—as opposed to the energy calculated as an integral of the spectral power within the same interval or energy of band-pass filtered signals. Difference between those estimates is explained in Figure 8. Choice of the gamma band between 35 and 38 Hz, based upon the overall picture from Figure 5, combined with such a selective energy estimate, increased the estimated gamma ERS above 4000%—double the result obtained via integration of the overall MP estimate between 36 and 40 Hz (Fig. 4).[2]

5 Discussion

Applying the proposed method basically confirms the classical results indicating different types of oscillations at a specific electrode location over the sensorimotor cortex. High resolution of the method results in an increased sensitivity to ERD and ERS. For example, by comparing Figures 4 and 3, we find that the maximum ERS in the gamma band, reaching 200% on the classical estimates in Figure 3, is an order of magnitude stronger when calculated in exactly the same way from the MP estimate of energy density. This result is doubled by a more adequate choice of the frequency interval, based upon the complete high-resolution picture of energy distribution, combined with a selective estimate of energy carried by structures originating within this frequency interval (Figure 7).

Detailed time-frequency information in Figure 5 allowed to distinguish two differently reacting oscillations within the alpha band: one component (10 Hz) showed only a weak attenuation with movement, whereas the other (between 11 and 11.5 Hz) was completely blocked. The 10 Hz component was found only in the referential recording (visible in Fig. 6) whereas the component above 11 Hz was clearly represented in the local reference (see Fig. 4). This can be explained by the effect of spatial high-pass filtering. The calculation of the local average reference results in damping of widespread activities around 10 Hz and in enhancing local activities around 11 Hz. Functional separation between lower and upper mu rhythm components has been suggested in [1].

Using the proposed procedure, it was further possible to study the time-frequency microstructure of beta and gamma bursts. Presented re-

[2]These numbers are quoted here only to illustrate the increase of sensitivity; *per se* they do not provide direct measures of the underlying phenomena. If we assume a complete absence of gamma in the reference period, their theoretical value would be infinite.

sults show consistently that the maximum of the gamma bursts occurred during maximal desynchronization of alpha and beta frequency components. In contrast to the conventional processing of the ERD/ERS by band pass filtering (Fig. 3), a more detailed structure of gamma components was obtained. The presence of movement-related gamma oscillations could even be demonstrated in referential data, when adequate time-frequency resolution was achieved.

Our experience gained with analysis of the data from other subjects indicates, that proposed method gives a generally applicable, robust and high-resolution estimates. It can be also naturally extended to a topographical analysis by comparison of results for simultaneously recorded derivations, as was presented e.g. in [14] for sleep spindles.

Software for matching pursuit with stochastic dictionaries, used in this research, is available from `http://brain.fuw.edu.pl/~mp`.

About the authors

Gert Pfurtscheller is Professor of Medical Informatics at Graz University of Technology, Director of the Institute of Biomedical Engineering at the University of Technology, and Director of the Ludwig Boltzmann Institute of Medical Informatics and Neuroinformatics. At present, he is involved in a number of research programs including the design of a "brain-computer interface," studies in functional brain topography using event-related desynchronization.

Christa Neuper is a Psychologist and a Research Assistant at the Ludwig Boltzmann Institute of Medical Informatics and at the Department of Medical Informatics, Institute of Biomedical Engineering, at Graz University of Technology. She teaches graduate courses at the Department of Psychology, University of Graz, since 1986, and at the Institute for Biomedical Engineering, Graz University of Technology, since 1996. Her research interests include the study of event-related oscillations in the brain, methodical aspects of EEG recording and processing, and neurophysiological applications.

Piotr J. Durka introduced adaptive approximations into the field of EEG analysis. As Assistant Professsor at the Warsaw University, he supervised M.Sc. thesis of Dobieslaw Ircha - implementation of stochastic dictionaries for MP. Current information on both of them is available from the Web page of the Laboratory of Medical Physics http://brain.fuw.edu.pl.

Cooperation which led to this paper from the very beginning was effectuated via Internet - the authors (from Poland and Austria) actually did not met in person. Email was the carrier for discussions, datasets, results, figures and finally the joint preparation of the manuscript.

References

[1] C. Andrew and G. Pfurtscheller. On the existence of different alpha band rhythms in the hand area of man. *Neurosci. Lett.*, 222:103–106, 1997.

[2] K.J. Blinowska, J. Ginter, P.J. Durka, D. Ircha, and W. Androsiuk. Time-frequency and topographic representation of movement planning. In *Abstracts of The First Joint Meeting of BMES & EMBS*, Atlanta, October 1999.

[3] P. J. Durka, D. Ircha, and K. J. Blinowska. Stochastic time-frequency dictionaries for matching pursuit. *IEEE Transactions on Signal Processing*, 49(3):507–519, March 2001.

[4] R. Elul. The genesis of the EEG. *International Review of Neurobiology*, 15:227–272, 1972.

[5] W. N. Kuhlman. Functional topography of the human mu rhythm. *Electroenceph. Clin. Neurophysiol.*, 44:83–89, 1978.

[6] S. Mallat and Z. Zhang. Matching pursuit with time-frequency dictionaries. *IEEE Transactions on Signal Processing*, 41:3397–3415, Dec 1993.

[7] G. Pfurtscheller and F. H. Lopes da Silva. Event-related EEG/MEG synchronization and desynchronization: Basic principles. *Clin. Neurophysiol.*, 110:1842–1857, 1999.

[8] G. Pfurtscheller, Ch. Neuper, and J. Kalcher. 40-hz oscillations during motor behavior in man. *Neurosci. Lett.*, 162/1-2:179–182, 1993.

[9] G. Pfurtscheller, A. Stancák, and Ch. Neuper. Post-movement beta synchronization. A correlate of an idling motor area? *Electroenceph. Clin. Neurophysiol.*, 98:281–293, 1996.

[10] Gert Pfurtscheller. EEG event-related desynchronization (ERD) and event-related synchronization (ERS). In E. Niedermayer and F. Lopes Da Silva, editors, *Electroencephalography: Basic Principles, Clinical Applications and Related Fields*, pages 958–965. Williams & Wilkins, fourth edition, 1999.

[11] S. Salenius, R. Salmelin, C. Neuper, G. Pfurtscheller, and R. Hari. Human cortical 40 hz rhythm is closely related to EMG rhythmicity. *Neurosci. Lett.*, 213:75–78, 1996.

[12] W. Singer. Synchronization of cortical activity and its putative role in information processing and learning. *Annu. Rev. Physiol.*, 55:349–374, 1993.

[13] G. W. Thickbroom, F. L. Mastaglia, W. M. Carroll, and H. D. Davies. Source derivation: application to topographic mapping of visual evoked potentials. *Electroenceph. Clin. Neurophysiol.*, 59:279–285, 1984.

[14] J. Żygierewicz, K.J. Blinowska, P.J. Durka, W. Szelenberger, Sz. Niemcewicz, and W. Androsiuk. High resolution study of sleep spindles. *Clin. Neurophysiol.*, 110(12):2136–2147, 1999.

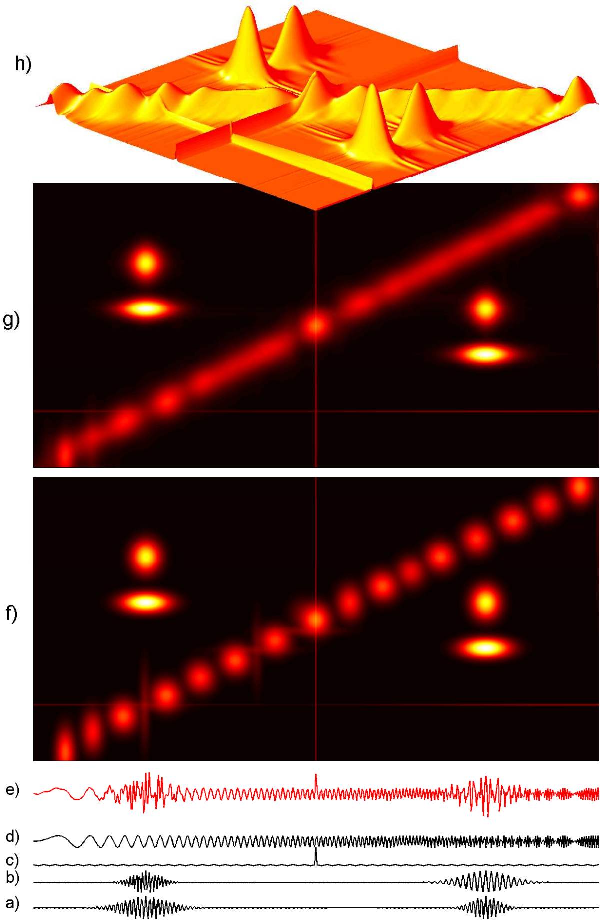

Figure 1: Time-frequency maps of energy density (eq. (5)) of a 500-points simulated signal (**e**) composed of four sine-modulated Gaussians, i.e. Gabor functions (**a**–**b**), sine wave and one-point discontinuity (**c**) and sine wave with linear frequency modulation—chirp (**d**). Distribution (**f**) was obtained from a single decomposition in a large ($2{*}10^6$ waveforms) dictionary: signal is described by only 30 functions, but changing frequency of the chirp is represented as a series of functions, since in the Gabor dictionary we have only constant frequency modulations. (**g**) presents average of 100 decompositions of the same signal in different realizations of smaller ($5 * 10^4$ atoms) stochastic dictionaries. This smoothes the representation of the chirp, but underlying parametrization is no more compact. (**h**)—the same as (g), presented in 3 dimensions. Square root of energy proportional to the height of the surface or "temperature" on 2-dimensional plots.

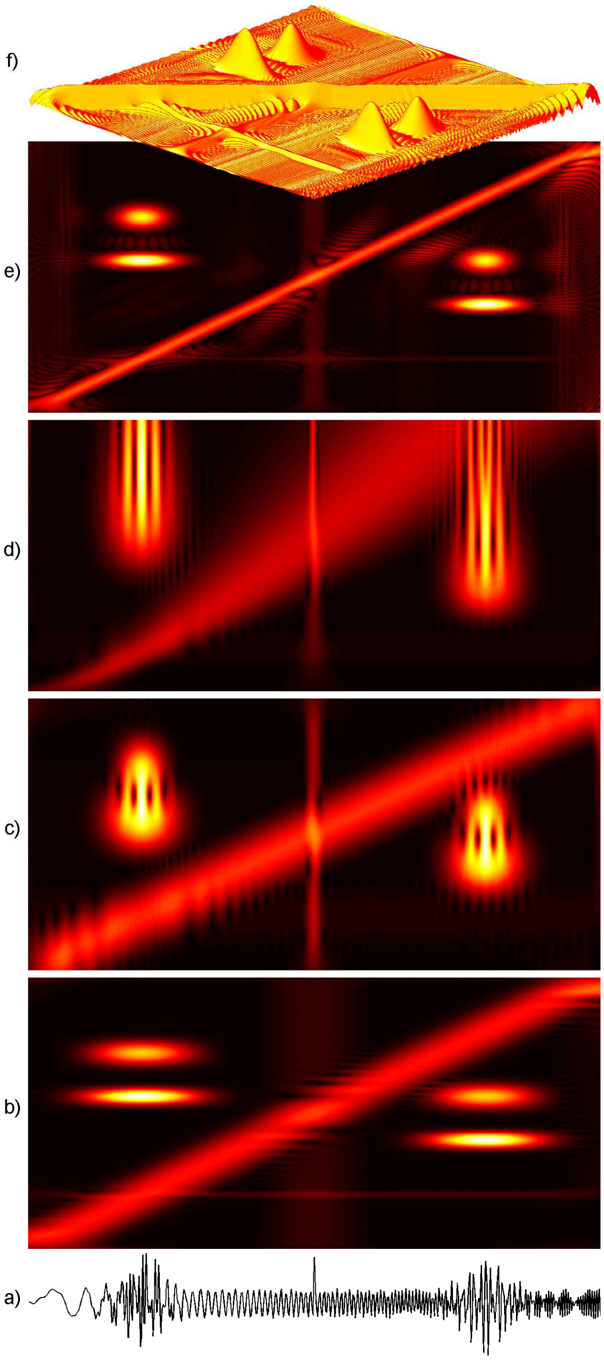

Figure 2: Time-frequency distributions of energy of the simulated signal (here plotted as **a**) from Figure 1. (**b**) and (**c**) present spectrograms (i.e. windowed or short-time Fourier transforms) calculated, respectively, for long (125 points) and short (21 points) windows. (**d**) is a scalogram (continuous wavelet transform), (**e**)—smoothed pseudo Wigner-Ville distribution, (**f**)—the same as (e) in 3 dimensions. Presentation as in Figure 1.

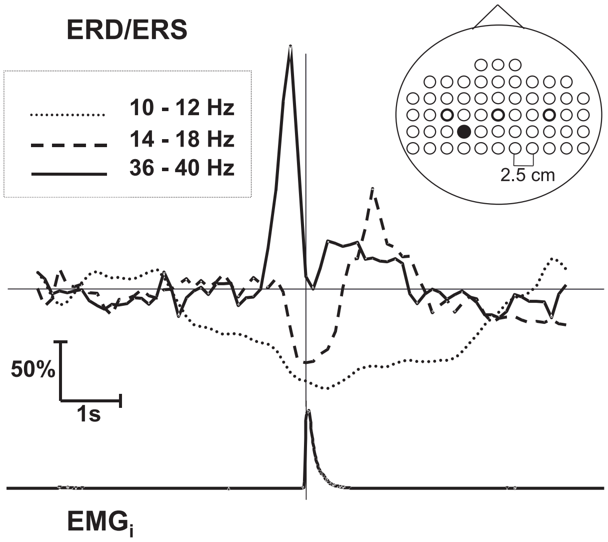

Figure 3: ERD/ERS in three bands: α 10-12 Hz, β 14-18 Hz, γ 36-40 Hz. Insert: electrode positions C3, Cz and C4 from the 10-20 system marked by thicker circles. Results presented for electrode marked by filled circle.

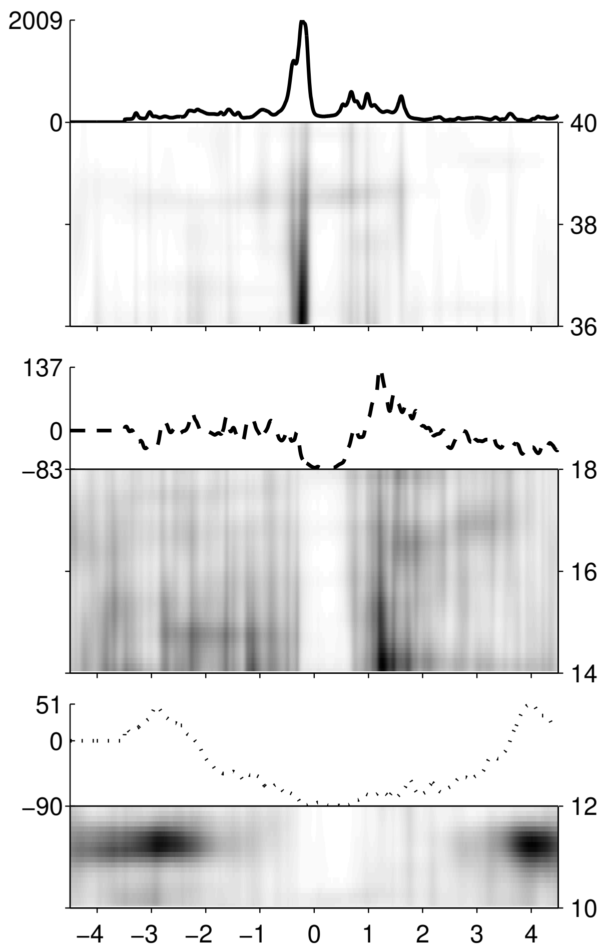

Figure 4: Average time-frequency maps of EEG energy density, obtained from the same data as analyzed in Figure 3. Horizontal axis—time in seconds relative to the finger movement. Vertical axes on the right of those maps indicate frequency in Hz. Energy proportional to shades of gray. Scale is arbitrary and different for each map. Curves above the maps, corresponding to figure 3, are frequency integrals of the maps below them. Vertical axes on their left sides indicate percent of change, relative to energy integrated between 3.5 and 4.5 seconds before the movement in given band.

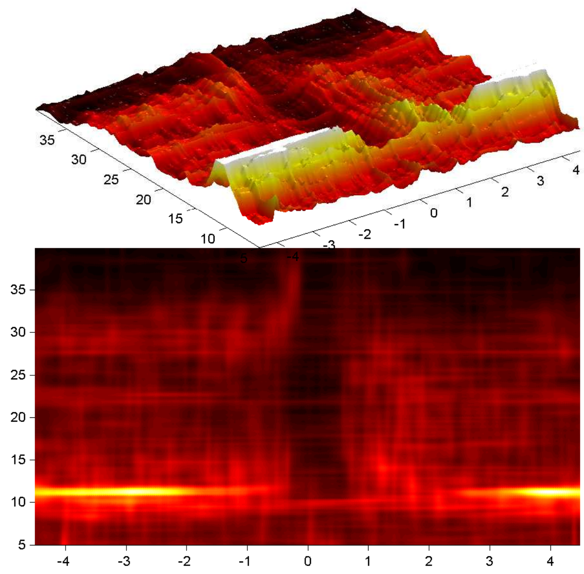

Figure 5: Complete time-frequency map (from 5 to 40 Hz), from which slices presented in Figure 4 were cut. Horizontal scale—seconds relative to the finger movement, vertical—frequency (Hz). Top—the same in 3 dimensions, but energy of the alpha band cut off in 50% of the height to show weaker high-frequency structures. Presentation as in Figure 1.

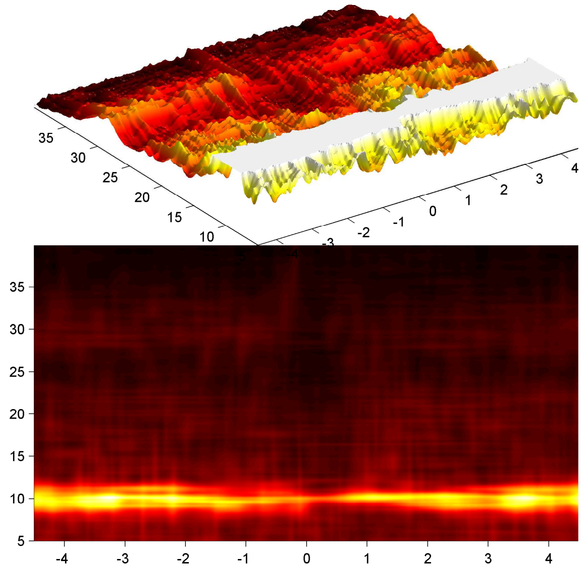

Figure 6: The same as Fig. 5, calculated for referential data. Alpha band energy in the 3-D plot cut at 25%.

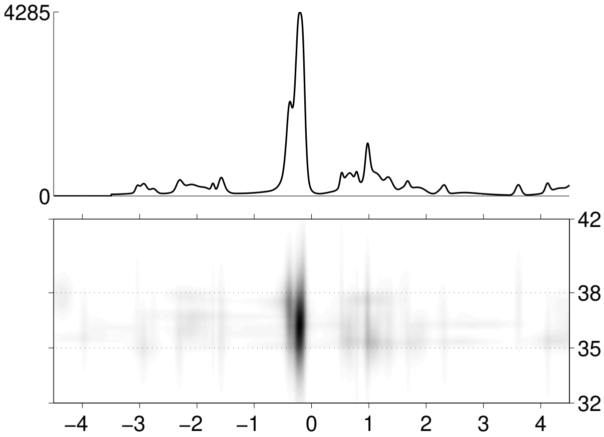

Figure 7: Bottom: time-frequency distribution of energy carried by structures with frequency centers lying between 35 and 38 Hz (interval chosen from the full picture of energy changes displayed in Figure 5). Top: gamma ERS based upon this estimate. Presentation as in Figure 4.

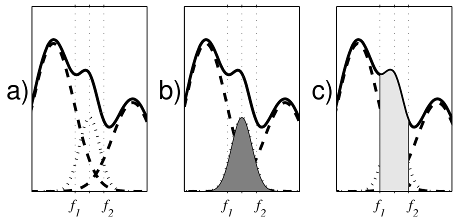

Figure 8: Difference between the spectral integral from f_1 to f_2 and the actual power carried by structures with frequency centers lying within this interval. Black solid line—spectrum resulting from the presence of three structures (spectra plotted with dotted and dashed lines in (**a**)). (**b**)—the actual power carried by the structure with frequency center between f_1 and f_2 (dark gray), (**c**)—spectral integral from f_1 to f_2. We observe that part of the energy originating within the interval spreads outside it, while part of energy of structures originating at outside frequencies contributes to the power integrated within the interval. Method proposed in this paper offers estimate corresponding to the dark area in (b). On the contrary, the classical estimate obtained via band-pass filtering is a smeared version of the light gray area in (c), since the band-pass properties of a filter are never perfect.